

7th INTERNATIONAL WORKSHOP ON NEW PHOTON-DETECTOR
BOLOGNA, ITALY
3–5 DECEMBER 2025

Photodetector and scintillators development for the LHCb ECAL upgrade

J. Delenne¹,^{a,b,*} E. Auffray,^a M. Barnyakov,^c A. Bellavista,^{c,d} A. Boayrintsev,^e
A. Carbone,^{c,d} F. Ferrari,^{c,d} Y. Hurkalkenko,^e D. Manuzzi,^c L. Martinazzoli,^a S. Perazzini,^c
M. Salomoni,^{a,f} V. Vagnoni,^c D. Yelisiev,^e F. Zenesini^c and P. Zhmurin^e

^aConseil Européen pour la Recherche Nucléaire (CERN),
Geneva, Switzerland

^bIPHC, UMR7178 CNRS, Université de Strasbourg,
Strasbourg, France

^cIstituto Nazionale di Fisica Nucleare (INFN),
Bologna, Italy

^dUniversità di Bologna,
Bologna, Italy

^eInstitute for Scintillation Materials (ISMA),
Kharkiv, Ukraine

^fUniversità degli Studi di Milano-Bicocca,
Milano, Italy

E-mail: julie.deleme@cern.ch

ABSTRACT. The LHCb electromagnetic calorimeter (ECAL) needs to be upgraded for Run 4 and 5, which will take place during the High-Luminosity phase of the Large Hadron Collider. The inner regions will be equipped with Spaghetti calorimeter (SpaCal) modules, using organic scintillating fibres in regions exposed to radiation doses of up to 200 kGy. A study has been carried out on plastic scintillators, focusing on green (3-hydroxyflavone (3HF)) and blue emitting plastic scintillators produced by ISMA in Kharkiv, Ukraine. Characterization of light yield, scintillation kinetics, and dedicated irradiation campaign have been performed, highlighting 3HF-based scintillators as promising candidates. In parallel, irradiation and ageing campaigns were performed on three Hamamatsu metal-channel dynode photomultiplier tubes (R9880U-20, R14755U-100 and R7600U-00-M4), considered as potential candidates for the upgrade. Tests up to 300 kGy and an integrated charge of about 1000 C were achieved, matching the expected operating conditions for LHCb Run 4 and Run 5.

KEYWORDS: Calorimeters; Radiation damage to detector materials (solid state); Photon detectors for UV, visible and IR photons (vacuum); Scintillators and scintillating fibres and light guides

*Corresponding author.

Contents

1	Introduction	1
2	R&D on scintillating plastics	1
2.1	Light yield	1
2.2	Scintillation time profile	2
2.3	Irradiation campaign	3
3	R&D on photodetectors	3
3.1	Irradiation campaign	3
3.2	Ageing studies	4
4	Conclusions	5

1 Introduction

During the High-Luminosity (HL) operation phase (Run 4 and Run 5) of the CERN Large Hadron Collider (LHC), the LHCb experiment is expected to operate at an instantaneous luminosity up to $1.5 \times 10^{34} \text{ cm}^{-2} \text{ s}^{-1}$, aiming at an integrated luminosity of 300 fb^{-1} . To cope with increased particle densities, the current electromagnetic calorimeter (ECAL), based on Shashlik modules, requires a substantial upgrade [1]. For Run 4 and Run 5, the LHCb ECAL will be upgraded, a new detector combining Shashlik and Spaghetti calorimeter (SpaCal) technologies to withstand high radiation levels while providing timing capabilities at the level of a few tens of picoseconds [2, 3]. In this design, SpaCal modules, based on scintillating fibres embedded in a dense absorber matrix, are foreseen for the innermost ECAL regions. SpaCal modules with plastic scintillators are planned for regions exposed to radiation doses of up to 200 kGy. This present study focuses on R&D on radiation-hard plastic scintillators with high light yield (above 6000 photons/MeV), required to preserve an energy resolution of 10. Plastics with a fast decay are investigated in order to achieve a time resolution of a few tens of picoseconds, helping to limit pile-up at the LHC with 25 ns bunch spacing. In addition, R&D on fast photodetectors is presented, targeting photomultiplier tubes (PMTs) capable of maintaining gain, quantum efficiency, and timing performance under the conditions expected for LHCb Run 4 and Run 5, with integrated charges up to 1000 C and radiation doses up to 300 kGy.

2 R&D on scintillating plastics

Several scintillator samples with a polystyrene (PS) matrix and different dyes, each in the form of a cylinder with a 10 mm^2 cross-section and 10 mm length, were produced by the Institute for Scintillation Materials (ISMA in Kharkiv, Ukraine) and characterized at CERN. They include four 3-hydroxyflavone (HF)-based green scintillators (labeled G1 to G4) and two blue ones: commercial UPS-932A (B1) and a highly polyphenylene-oxide-doped sample (B2).

2.1 Light yield

The light yield was measured using a Hamamatsu R2059 photomultiplier tube (PMT) coupled to a CAEN DT5720 digitizer in charge integration mode. Each scintillator was wrapped in Teflon, optically

coupled to the PMT with glycerine and excited by a ^{137}Cs source (661.7 keV γ -rays). The light yield was extracted by fitting the Compton edge (477.3 keV) of the integrated charge spectrum, calibrated with the PMT single-photoelectron peak and corrected using the quantum efficiency (QE) weighted over the scintillator emission spectrum. Figure 1 (left) shows the distribution of the photons detected after exciting the scintillators with a ^{137}Cs source. The light yield values are summarized in table 1. All green-emitting samples exhibit light yields above 5000 photons/MeV, whereas the blue-emitting B2 sample shows a particularly bright emission of 10 623 photons/MeV.

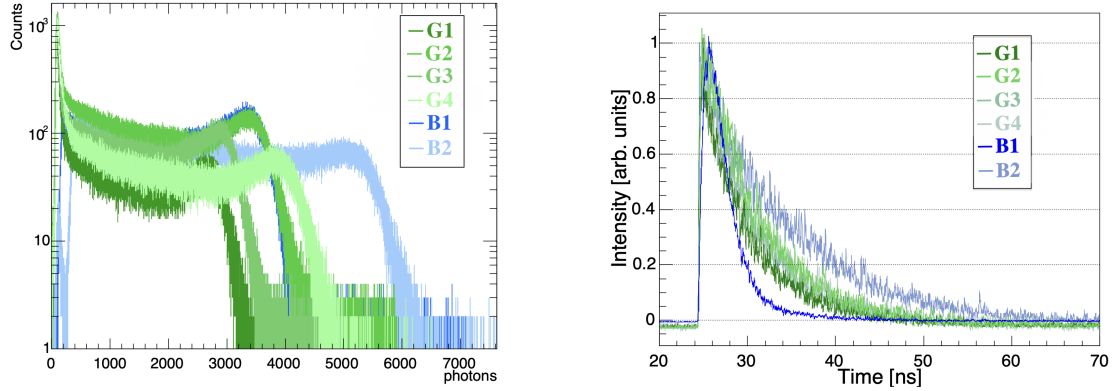


Figure 1. Detected photon distribution from plastic scintillators excited by a ^{137}Cs source (left), scintillation decay time profiles of the investigated plastic scintillators (right).

Table 1. Summary of the experimental results: emission peak wavelength, light yield ($\pm 5\%$) extracted from the 477.3 keV Compton edge of a ^{137}Cs source, scintillation time profile fit, effective decay time, and induced absorption coefficient at the emission peak for two radiation doses.

Label	Emission peak [nm]	Light yield [photon/MeV]	R1 τ_{d1}		R2 τ_{d2}		τ_{eff} [ns]	μ_{ind} [m^{-1}]	
			[ns]		[ns]			@ 50 kGy	@ 300 kGy
G1	529	5522	0.41	3.90	0.59	8.10	5.6	8.47	15.7
G2	527	7061	0.92	6.42	0.08	29.0	6.8	A	39.5
G3	538	6017	0.79	5.15	0.21	13.7	5.9	10.9	63.9
G4	537	7994	0.09	0.55	0.91	7.38	3.5	15.8	58.7
B1	420	6922	0.90	1.96	0.10	5.60	2.1	32.8	195.3
B2	434	10623	1.00	11.4			11.4	A	64.3

A = anomaly observed in the sample

2.2 Scintillation time profile

The scintillation emission-time distribution of the samples is measured using a Time Correlated Single Photon Counting (TCSPC) setup, as described in detail in [4]. The decay time profile was modeled as follows:

$$f(t) = \sum_{i=1}^2 R_i \cdot \frac{\exp\left(-\frac{t-\theta}{\tau_{d,i}}\right) - \exp\left(-\frac{t-\theta}{\tau_{r,i}}\right)}{\tau_{d,i} - \tau_{r,i}} \cdot \Theta(t - \theta) \quad (2.1)$$

where $\tau_{d,i}$ and $\tau_{r,i}$ are, respectively, the i th component of the decay and rise time constants, R_i is the weight of the i th component, and θ is the instant above which the scintillation pulse starts. All decay

profiles were fitted with two components, except B2, fitted with a single component. The effective decay time is calculated as the weighted harmonic average $\tau_{\text{eff}} = ((R_1/\tau_{d,1}) + (R_2/\tau_{d,2}))^{-1}$. The decay time profiles of the plastic scintillators are shown in the figure 1 (right), and the parameters extracted from equation (2.1) are summarized in table 1. The decay time components obtained for G2, approximately 7 ns and 30 ns for its first and second components, respectively, are in agreement with the usual values reported for 3HF-based scintillators [5]. The other green-emitters are faster, with G4 exhibiting a very fast dominant decay and no component around 30 ns, which results in a shorter effective decay time of 3.5 ns compared to 7 ns for G2. A correlation between light yield and decay time is observed for G1, G2, and G3, with faster samples exhibiting lower light yield. G4 combines high light yield with fast kinetics, making it promising for timing applications. For the blue emitters, B1 shows a fast response with an effective decay time of 2.1 ns, whereas B2 is significantly slower, with an effective decay time of about 11 ns.

2.3 Irradiation campaign

An irradiation campaign was conducted at the CERN IRRAD proton facility where samples were exposed to a primary proton beam with a momentum of 24 GeV/c. Each scintillator type was irradiated at two fluences: 1.6×10^{14} protons/cm² (approximately 50 kGy) and 9.6×10^{14} protons/cm² (approximately 300 kGy). The transmittance of the samples was measured before (T_b) and one month after irradiation (T_a) using a PerkinElmer LAMBDA 650 UV/VIS spectrometer. Radiation-induced optical changes were quantified using the induced absorption coefficient, defined as $\mu_{\text{ind}} = \ln(T_b/T_a)/L$, where L is the sample thickness. The induced absorption coefficients at the emission peak for the two doses are reported in the table 1. It is observed that the radiation damage measured for green emitters is lower than blue emitters. Indeed, fluoroderivatives of 3HF emit at longer wavelengths, allowing excitation-energy traps (generally in the blue region) to be bypassed and improving the radiation hardness. Among the green emitters, G1 presents better radiation tolerance, with induced absorption after 300 kGy four times lower than the other samples. Moreover, the ratio between induced absorption after 50 kGy and 300 kGy for G1 is two times lower compared to a factor of four to six lower for the other samples, which indicates that the saturation is reached faster.

3 R&D on photodetectors

3.1 Irradiation campaign

Metal channel dynodes (MCDs) provide excellent timing performance and are therefore potential candidates for the LHCb Upgrade II [2]. In this study, two R14755U-100, two R9880U-20, and two R7600U-00-M4 Hamamatsu PMTs were investigated. An additional R7600U-00-M4 was used as a reference. A PMT irradiation campaign was carried out at the CERN IRRAD proton facility. All six PMTs were first exposed to a fluence of 3.67×10^{14} protons/cm² (approximately 150 kGy), and then three PMTs (one of each type) were further irradiated to an additional fluence of 3.83×10^{14} protons/cm², reaching a total dose of about 300 kGy. After irradiation, the PMTs were characterized by illuminating the center of the photocathodes with an UV LED ($\lambda \approx 380$ nm). The HV dividers were modified to allow photocurrent measurements. Figure 2 shows the photocathode currents of the irradiated PMTs, normalized to that of the reference PMT, reflecting the changes in quantum efficiencies. The first 150 kGy irradiation reduced the photocurrent by a factor of 2.0–2.7, with no additional degradation upon the second exposure. A partial recovery of the sensitivity, ranging

from 17% to 28%, was observed after approximately three months of rest. Following irradiation, the PMT gain remained stable within $\pm 10\%$. The QE degradation by a factor of about 2.3 on average is consistent with previous measurements of the radiation-induced darkening of the PMT borosilicate window. The impact of the observed QE degradation on the SpaCal performance is not negligible, and a strategy to mitigate this effect needs to be developed.

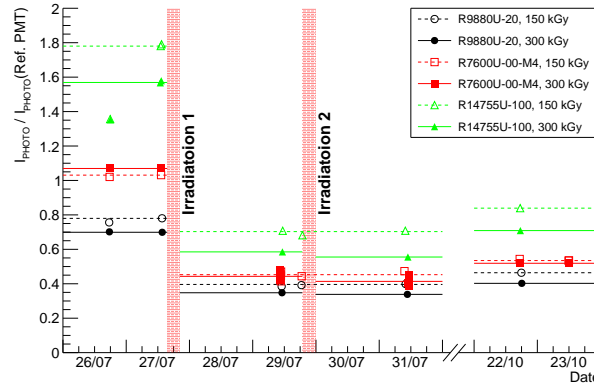


Figure 2. Photocathode currents of six PMTs, normalized by a non-irradiated R7600U-00-M4.

3.2 Ageing studies

An ageing campaign was carried out on R14755U-100 and R9880U-20 PMTs, which had not been subjected to any irradiation and whose cell size matches the SpaCal modules. The PMTs were continuously illuminated with a white LED for 160 days, corresponding approximately to an integrated anode charge of 1100 C. For PMT characterization, the LED was switched off and a 405 nm picosecond diode laser was used. The evolution of the anode sensitivity during the ageing campaign for both PMTs is shown in figure 3 (left). Both PMTs exhibit a rapid drop during the first 50 C, followed by a gradual decrease to 40–50% of the initial level at the end of the ageing. For R9880U-20, the photocurrent was also measured, that allowed us to separate the contributions of gain and QE changes to the anode sensitivity degradation (see figure 3 right). The gain shows a 30% reduction up to 50 C, after which it remains stable. No significant QE degradation is observed within the first 200 C, but it subsequently decreases by about 30%.

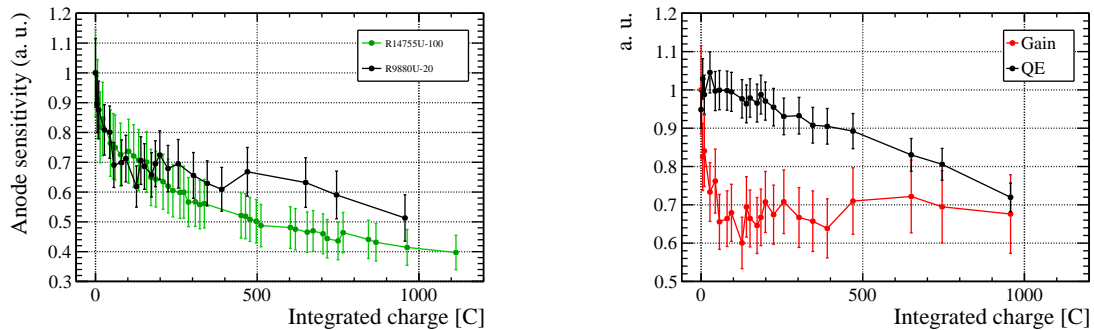


Figure 3. Variation of the anode sensitivity (normalized by the maximum) during the ageing campaign performed at 500 V (left), and the gain and QE measured at 405 nm for R9880U-20 (right).

4 Conclusions

In summary, ongoing R&D efforts focus on developing radiation-hard calorimeter components for LHCb Upgrade II, targeting sufficient light yield, fast timing, and stable performance under Run 4 and Run 5 conditions. Chemical composition studies indicate that 3HF derivative exhibited promising optical and timing performance. G4 and B1 show high light yield and fast scintillation kinetics but limited radiation tolerance. G1 demonstrates the best radiation hardness among all samples, though its light yield remains below 6000 photons/MeV, which may impact the energy resolution. In contrast, G4 and B1 provide higher light yield and faster decay but lower radiation tolerance.

For photodetectors, an irradiation campaign was performed on three types of Hamamatsu PMTs, with doses up to 300 kGy, corresponding to the expected conditions for LHCb Run 4 and Run 5. The campaign showed a decrease in QE due to window darkening, while the gain remained unchanged within $\pm 10\%$. An ageing campaign was carried out with R9880U-20 and R14755U-100, reaching approximately 1100 C of integrated charge over 160 days, matching the expected operational conditions. During this test, the anode sensitivity decreased in 2.0–2.5 times. Half of this degradation is due to the gain drop and can be recovered by voltage increase.

Acknowledgments

Part of this work has been carried out in the framework of EP R&D and the Crystal Clear Collaboration and received support from EP R&D and the Horizon Europe ERA Widening Project no. 101078960 “TWISMA”. The work contained in this paper is supported also by the Italian Ministero dell’Università e Ricerca (MUR) and European Union - Next Generation EU through the research grant number 2022MHC2MH, CUP I53D23001310006, under the program PRIN 2022.

References

- [1] LHCb collaboration, *LHCb Particle Identification Enhancement*, [LHCb-TDR-024](#) (2024).
- [2] LHCb collaboration, *LHCb Upgrade II Scoping Document*, [LHCb-TDR-026](#) (2024).
- [3] L. An et al., *Performance of a spaghetti calorimeter prototype with tungsten absorber and garnet crystal fibres*, *Nucl. Instrum. Meth. A* **1045** (2023) 167629 [[arXiv:2205.02500](#)].
- [4] F. Pagano et al., *A new method to characterize low stopping power and ultra-fast scintillators using pulsed X-rays*, *Front. Phys.* **10** (2022) 1021787.
- [5] Y.A. Gurkalenko, *The plastic scintillator activated with fluorinated 3-hydroxyflavone*, *Funct. Mater.* **24** (2017) 005.